Photoelectron spectroscopy of the negative cluster ions $NO^-(N_2O)_{n=1,2}$

J. V. Coe, J. T. Snodgrass, C. B. Freidhoff, K. M. McHugh, and K. H. Bowen
Department of Chemistry, The Johns Hopkins University, Baltimore, Maryland 21218

(Received 9 January 1987; accepted 10 July 1987)

We have recorded the photoelectron (photodetachment) spectra of the gas-phase negative cluster ions $NO^-(N_2O)_1$ and $NO^-(N_2O)_2$ using 2.540 eV photons. Both spectra exhibit structured photoelectron spectral patterns which strongly resemble that of free NO^-, but which are shifted to successively lower electron kinetic energies with their individual peaks broadened. Each of these spectra is interpreted in terms of a largely intact NO^-subion which is solvated and stabilized by nitrous oxide. For both $NO^-(N_2O)_1$ and $NO^-(N_2O)_2$, the ion–solvent dissociation energies for the loss of single N_2O solvent molecules were determined to be $\sim$0.2 eV. Electron affinities were also determined and found to increase with cluster size. The localization of the cluster ion's excess negative charge onto its nitric oxide rather than its nitrous oxide subunit is discussed in terms of kinetic factors and a possible barrier between the two forms of the solvated ion.

I. INTRODUCTION

Negatively charged atomic and molecular cluster ions have counterparts in every phase of matter. Cluster ions are often the energetically preferred form of ions in relatively cool gaseous media, and both positive and negative cluster ions are known to be important in the ion–molecule chemistry of the upper atmosphere.[1] Under some circumstances, cluster ion-induced nucleation may play a role in the conversion of vapors into macroscopic air-borne particulates, such as aerosols and soot.[2] Cluster ions are also responsible for the charged tracks seen in the wake of ionizing radiation which has passed through cloud chambers. Ion-induced nucleation mechanisms have even been proposed for the formation of interstellar dust. In solution, solvated ions govern a host of phenomena including solvent dependent variations in the reactivity and spectral characteristics of anions[3] and cations. In addition to solvated negative ions, solvated electrons are yet another class of negative cluster ion analogs found in liquids.[4] These unique species are collective state entities in which the excess electron is delocalized over the immediate solvent environment. Counterparts to negative cluster ions are also found in the solid phase, and these include trapped electron states which exist as imperfections in crystals and negative ions which have been condensed along with neutrals into cryogenic matrices. Perhaps more importantly, however, negative cluster ions may also lead us to the electron affinities of neutral clusters which may themselves be useful model systems in the study of solids and their surfaces. Aggregated states of matter lying in the transitional size regime between an isolated atom or molecule and the condensed phase have been the subject of considerable interest in part because their evolving electronic properties are important measures of when clusters or aggregates have become large enough to be considered pieces of bulk liquid or solid.[5] Furthermore, the differing electronic properties of small, aggregate-like regions on surfaces are thought to be influential in affecting chemisorption, surface reactivity, and the characteristics of thin films and other microstructures.

The importance of negative cluster ions to so many basic processes and phenomena together with the difficulties involved in resolving and characterizing the roles of individual anionic species in condensed phases has led to the development of a variety of methods for generating and studying negative cluster ions in the gas phase. Chemically diverse beams of negative cluster ions have been produced in several types of ion source environments using charged-particle beam (e^-,H^+,Cs^+) bombardment,[6–10] electrical discharges,[11,12] radioactivity,[13] photoemission of electrons,[14] laser vaporization,[15] and collisional charge transfer[16] as methods of ionization. Experimental studies of negative cluster ions have included thermochemical measurements,[17–19] determinations of reactive rate constants,[20] electron attachment studies,[21,22] photodestruction cross section measurements,[23,24] photodissociation experiments,[25] and photodetachment studies.[26–32] Theoretical work on negative cluster ions has addressed a wide range of issues. Topics as diverse as negative ion solvation,[33,34] trapped and solvated electron states,[35] and the variation of metal cluster electron affinities with cluster size[36,37] have all received substantial attention by theorists. As a result of both experimental and theoretical work on this subject there now exists a healthy data base of rate constant and thermochemical information, an enticing set of energetic and structural predictions provided by theory, and the beginnings of spectroscopic studies on negative cluster ions.

This paper is the third in a series[27,28] which reports the application of negative ion photoelectron (photodetachment) spectroscopy to the study of negative cluster ions. Negative ion photoelectron spectroscopy is conducted by crossing a mass-selected beam of negative ions with a fixed-frequency photon beam and energy analyzing the resultant photodetached electrons. Subtraction of the center-of-mass electron kinetic energy of an observed spectral feature from the photon energy gives the transition energy (the electron binding energy) from an occupied level in the negative ion to an energetically accessible level in the corresponding neutral. This technique has been applied to a wide variety of small unclustered negative ions, and in addition to electron

 0021-9606/87/204302-08$02.10

affinities, it has provided vibrational frequencies for the ions and their neutrals, electronic splittings in the neutrals, and geometrical information.[38,39]

In the work described here we have obtained the structured photoelectron spectra of the negative cluster ions, $NO^-(N_2O)_1$ and $NO^-(N_2O)_2$. These experiments were undertaken as part of our broader effort to (a) explore the variation of cluster electron affinities and cluster ion dissociation energies with cluster size and (b) to illuminate some of the main features of the bonding in negative cluster ions. This paper reports on progress in both of these areas.

II. EXPERIMENTAL

A. Apparatus

Our negative ion photoelectron spectrometer has been described previously.[40] Here, we present only brief descriptions of its three main component systems. These are (a) the beam line along which negative ions are formed, transported, and mass selected, (b) the high-power argon ion laser operated intracavity in the ion–photon interaction region, and (c) the doubly magnetically shielded, high resolution hemispherical electron energy analyzer which is located below the plane of the crossed ion and photon beams.

The beam line originates at the ion source and terminates at a Faraday cup beyond the ion–photon interaction region. Cylindrical three element electrostatic lenses and electrostatic deflectors are used to transport the ions through the four separately pumped vacuum chambers of the apparatus. The mass selector is a cooled Colutron 600B Wien filter. This is a E x B velocity filter with electrostatic shims which compensate for the focusing effects of simple Wien filters. Mass selection allows us to "purify" our starting sample of negative ions before photodetachment and thus to obtain interference-free photoelectron spectra of specific negative ions. This capability is well suited for studies of homologous series of ions such as negative cluster ions.

The laser is a Spectra Physics model 171-18 argon ion laser which is operated intracavity by replacing its front mirror with a set of highly reflective mirrors to extend the cavity through the ion–photon intersection region. The laser is most often operated on its 488 nm line and achieves a typical power of $\sim$150 circulating watts with a plasma tube discharge current of 35 A. The laser housing is mounted so that the laser's polarization vector makes an angle of approximately 55° with the electron collection direction. This insures that the angular portion of the differential cross section for photodetachment vanishes so that the measured peak intensities in our spectra are proportional to the total photodetachment cross section.

The electron energy analyzer consists of three main parts: electron injection optics, energy dispersing elements, and electron output optics. The injection optics consist of two electrostatic three cylinder lenses and a pair of deflectors. The first electron lens adds energy to all the electrons such that those being counted have 20 times their original kinetic energy. The second lens is operated as a zoom lens and images the electrons from the first lens at the input plane of the energy dispersing elements with constant energy. The energy dispersing elements are OFHC copper hemispheres with a radius of 8.890 cm and a gap of 1.905 cm. The output electron optics consist of a single three cylinder lens and a pair of deflectors. The output lens images the hemisphere's output onto an 0.07 cm diam molybdenum aperture. Electrons which pass through this aperture are accelerated to 300 eV and impinge onto the front of a Ceratron electron multiplier.

B. Production of $NO^-(N_2O)_n$

Beams of $NO^-(N_2O)_n$ were generated in a supersonic expansion-ion source similar to that developed by Haberland.[41] Figure 1 presents a schematic of our version of this source. In this source a biased filament located just outside the nozzle orifice injects relatively low energy electrons into the supersonic expansion. Typical operating conditions during these experiments were: a nozzle stagnation pressure of $\sim$2 atm (neat N_2O), a nozzle diameter of 18 μm, a source beam voltage of $-$ 800 V, a filament bias voltage of $-$ 40 V relative to the source, a filament emission current of 25 mA, and a nozzle housing temperature of $\sim$200 K. Permanent magnets placed near the expansion jet were found to enhance the production of negative ions. Under these expansion conditions, neutral clusters of nitrous oxide were probably being generated in abundance. A typical mass spectrum showing the negative ions produced under these circumstances is presented in Fig. 2. The complex ions observed include $O^-(N_2O)_n$, $NO^-(N_2O)_n$, and $(N_2O)_n^-$. Negative ions with masses corresponding to $O^-(N_2O)_n$, $NO^-(N_2O)_n$ and N_2O^- have also been observed by other investigators.[21,42–44]

Hot cathode discharge (Branscomb)[45] ion sources have often been the workhorse of negative ion beam experiments. It is thus of interest to compare some of the characteristics of the relatively new nozzle-ion source with those of the more commonly used Branscomb source. When nitrous oxide is employed as a source gas the Branscomb source typically generates strong and roughly comparable intensity beams of O^-, NO^-, O_2^-, and NO_2^-. With the same source gas the nozzle-ion source produces strong beams of O^- and NO^-, greatly attenuated beams of O_2^- and NO_2^-, weak beams of N_2O^-, and as already described three different homologous series of cluster ions. While the ions O^- and NO^- can be formed directly from N_2O, the ions O_2^- and NO_2^- require subsequent ion–molecule reactions to be formed. We surmise that while these can occur readily in the 0.1–0.5 Torr environment of a Branscomb source, they can not in a nozzle expansion due to its relatively rapid transition to low density conditions. Also, based on an analysis of hot bands in negative ion photoelectron spectra, the vibrational "temperatures" of negative ions generated in Branscomb sources are usually $\sim$800 K. Photoelectron spectra of O_2^-, generated in our nozzle-ion source with neat O_2 as the source gas, indicate that the vibrational temperature of O_2^- can be varied by changing source conditions and that the temperature usually attained is somewhat cooler, typically 400–500 K. Presumably, cluster ions generated by a nozzle-ion source would be cooler than this since low-frequency cluster vibrational modes would be expected to relax more efficiently in a free jet expansion than the higher frequency vibration of O_2^-.

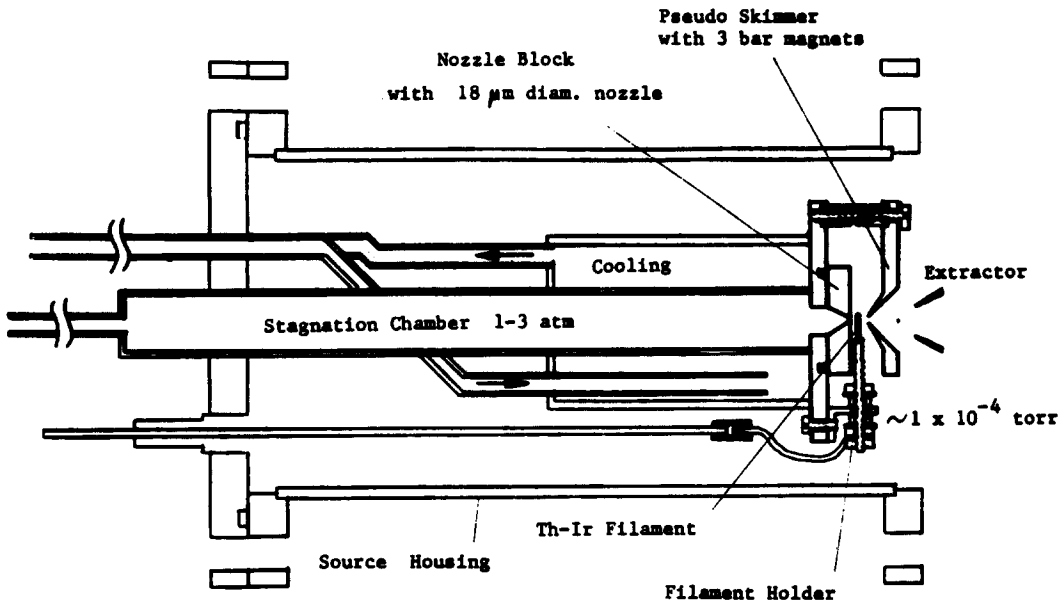

FIG. 1. The supersonic nozzle-ion source used in these experiments.

III. RESULTS AND INTERPRETATION OF SPECTRA

A. Data

The negative ion photoelectron spectra of NO^-, $NO^-(N_2O)_1$, and $NO^-(N_2O)_2$ are presented in Fig. 3. In all of these spectra the channel spacing was 8.5 meV, the photon energy was 2.540 eV, the laser power was ~175 circulating watts, and the analyzer's instrumental resolution was 30 meV. The NO^- spectrum was taken with 1.1×10^{-9} A of ion current, the $NO^-(NO)_1$ spectrum with 0.3×10^{-9} A, and the $NO^-(N_2O)_2$ spectrum with 0.04×10^{-9} A. The photoelectron spectra of NO^- and O^- are well known,[46,47] and both were taken before and after every negative cluster ion spectrum for calibration purposes. All peaks were fit in a

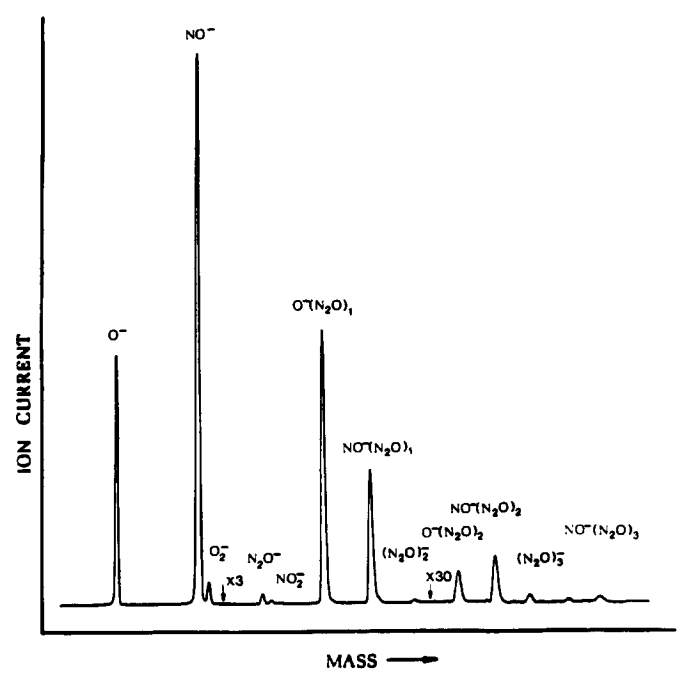

FIG. 2. A mass spectrum showing the negative ions produced by our nozzle-ion source when neat nitrous oxide was used as the feed gas. The ion current in this mass spectrum was measured at a Faraday cup located downstream of the ion–photon interaction region.

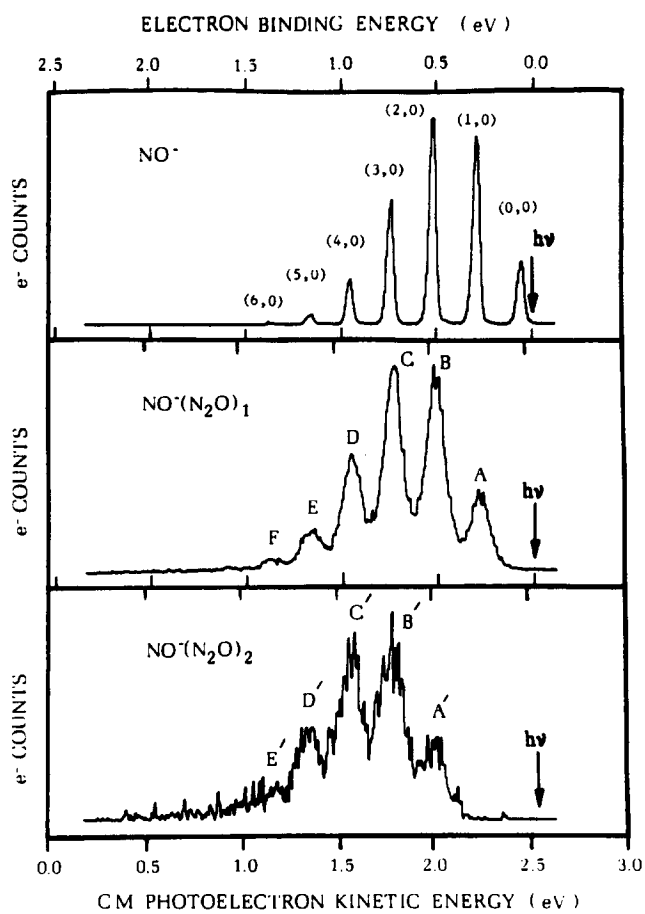

FIG. 3. The negative ion photoelectron spectra of NO^-, $NO^-(N_2O)_1$, and $NO^-(N_2O)_2$ all presented on the same center-of-mass electron kinetic energy and electron binding energy scales to facilitate comparison. All three spectra were recorded using 2.540 eV photons.

nonlinear least squares sense to the functional form of an asymmetric Gaussian. The center-of-mass electron kinetic energies, peak spacings, relative intensities, peak widths, and assignments are presented in Table I. Also, Fig. 2 shows the mass resolution that was typically utilized during these experiments. Under these circumstances the photoelectron spectrum of NO^- showed no interference due to the spectrum of O_2^- and vice versa. We are therefore confident that mass selection and discrimination in these experiments was quite good, and that mass "leakage" of unwanted ions into the ion–photon interaction region was minimal.

B. Characterization as $NO^-(N_2O)_n$

An important aspect of ion–neutral bonding concerns the distribution of excess negative charge over the negative cluster ion. One can imagine two extreme charge distribution categories where in one the excess charge is localized on a single component of the cluster ion, and where in the other there is a dispersal of the negative charge over part or all of the cluster ion. The situation where the excess charge is localized on a single component of the cluster ion is reminiscent of the usual notion of a solvated anion in which a cental negative ion is surrounded by a sheath of neutral solvent molecules. There the central negative ion may be thought of as remaining largely intact even though it is perturbed by its solvents. In this case electrostatic interactions between the ion and the solvent molecules presumably dominate the bonding. In other cases, however, charge dispersal effects may also make significant contributions to the bonding. These contributions may arise either in the sense of covalency in ion–neutral bonds or in the sense of excess electron delocalization via electron tunneling between energetically and structurally equivalent sites within the cluster ion. In favorable cases the photoelectron spectra of negative cluster ions can offer clues as to the nature of the excess charge distribution in these species.

The two ions that we have studied in this work have the stoichiometric formulas, $N_3O_2^-$ and $N_5O_3^-$. Evidence for characterizing them as $NO^-(N_2O)_1$ and $NO^-(N_2O)_2$, respectively, comes both from our mass and our photoelectron spectra. In addition to other negative ions, our mass spectrum (Fig. 2) exhibits a sequence of ionic species at masses 30, 74, 118, and 162 amu. The ions of this sequence originate at NO^-, are spaced by 44 amu, and decrease monotonically in intensity with increasing mass. Except for NO^- we do not observe these ions when using nitrous oxide in Branscomb sources. It appears that they are formed only in source environments which are conducive to cluster ion formation, e.g., ion drift tubes and ion sources which utilize supersonic expansions. Taken together this evidence suggests a homologous series of negative cluster ions, probably $NO^-(N_2O)_n$ but conceivably $N_3O_2^-(N_2O)_{n-1}$ where $N_3O_2^-$ denotes the possibility of an unclustered chemically bound ion of that stoichiometry. The photoelectron spectra discussed below distinguish between these possibilities and strongly support the characterization of this ionic sequence as $NO^-(N_2O)_n$.

The nomenclature $NO^-(N_2O)_n$ implies that an intact NO^- ion interacts with or is solvated by neutral N_2O molecules; which is to say that the excess negative charge is essentially *localized* on the nitric oxide component of the cluster ion. In this solvated-ion (ion–molecule complex) bonding picture the perturbed NO^- subion might be expected to act as the "chromophore" for photodetachment. This in turn would lead to a photoelectron spectrum of the $NO^-(N_2O)_n$ cluster ion that resembled the photoelectron spectrum of free unperturbed NO^- except for its features being shifted to lower electron kinetic energies (corresponding to increased

TABLE I. Electron energies, spacings, widths, intensities, and assignments of peaks.

c.m. electron kinetic energies of peak centers (eV)	Spacing between adjacent peaks (eV)	FWHM (eV)	Relative intensities	Assignment (v',v'')
		NO^-		
2.503		0.042	392	(0,0)
2.268	0.235	0.041	1191	(1,0)
2.039	0.229	0.040	1303	(2,0)
1.814	0.225	0.039	724	(3,0)
1.595	0.219	0.040	253	(4,0)
1.381	0.214	0.041	55	(5,0)
		$NO^-(N_2O)_1$		
2.282 (A)		0.122	207	(0,0)[a]
2.051 (B)	0.231	0.126	528	(1,0)
1.819 (C)	0.232	0.133	550	(2,0)
1.602 (D)	0.217	0.132	312	(3,0)
1.374 (E)	0.228	0.161	110	(4,0)
1.150 (F)	0.224	0.118	33	(5,0)
		$NO^-(N_2O)_2$		
2.027 (A')		0.136	29	(0,0)[a]
1.798 (B')	0.229	0.165	64	(1,0)
1.592 (C')	0.206	0.164	63	(2,0)
1.361 (D')	0.231	0.166	34	(3,0)
1.137 (E')	0.224	0.320	10	(4,0)

[a] Assignments are with respect to photodetachment of the NO^- subion.

stabilization) and perhaps broadened.

The photoelectron spectra of NO^-, $NO^-(N_2O)_1$, and $NO^-(N_2O)_2$ are all plotted in Fig. 3 on the same center-of-mass electron kinetic energy scale to facilitate comparison. The photoelectron spectrum of NO^- is well known, NO^- having been the first molecular negative ion to be studied by negative ion photoelectron spectroscopy.[46] When an electron is attached to NO to form NO^-, it is accommodated in an antibonding orbital of NO, and the nitrogen–oxygen bond distance increases. Given the geometrical difference between the ion and its corresponding neutral, the photoelectron spectrum of NO^- is a simple vibrationally resolved envelope which exhibits (v',v'') transitions between the $v''=0$ vibrational level of NO^- and the $v'=0$–6 vibrational levels of NO. Transitions from higher v'' levels of NO^- are not observed because these are autodetaching.

The most striking observation to make about the photoelectron spectra of $NO^-(N_2O)_1$ and $NO^-(N_2O)_2$ is that the spectral pattern or profile of free NO^- is preserved in both of them. The NO^- spectral patterns evident in these spectra are simply shifted to successively lower electron kinetic energies with their individual peaks broadened. As is discussed further in Sec. III D, the observed spectral patterns in both the $NO^-(N_2O)_1$ and the $NO^-(N_2O)_2$ photoelectron spectra are quantitatively very similar to that of the NO^- spectrum. Strictly speaking, this implies that the neutral form of the negative ion species being photodetached has a vibrational frequency which is very close to that of NO, and that the structural relationship between the photodetached ion and its corresponding neutral is much like that between NO^- and NO. In other words, there is good reason to interpret the photoelectron spectra of masses 74 and 118 as those of slightly *perturbed* NO^-. In the case of the species at mass 74, NO^- is perturbed by its interaction with a single N_2O solvent molecule, and in the case of mass 118, it is perturbed by two N_2O solvents. We find no evidence for the photodetachment of negative charge from the nitrous oxide portion of the cluster ion. We have recently recorded the photoelectron spectra[28] of N_2O^- and of $(N_2O)_2^-$, and we find no pertinent similarities between these and the $NO^-(N_2O)_{n=1,2}$ spectra. Thus, the negative ion photoelectron spectra have substantiated the nomenclature $NO^-(N_2O)_n$ by providing strong evidence that the excess negative charges on $N_3O_2^-$ and $N_5O_3^-$ are largely localized on NO^- subions which are themselves solvated by one and by two N_2O molecules, respectively. Implicitly, these results also show that it is very unlikely that the homologous cluster ion series being studied here is $N_3O_2^-(N_2O)_{n-1}$, or that $NO^-(N_2O)_1$ is actually $NO_2^-(N_2)_1$. (The EA of NO_2 is 2.275 eV.[48])

C. Energetics

The reactants and products of the photodetachment process are, respectively, negative ions and photons, and neutrals and free electrons. The energetic relationships between the generic negative cluster ions, $A^-(B)_n$, and their corresponding neutral clusters, $A(B)_n$, are expressed through the identities,

$$\mathrm{EA}[\mathrm{A(B)}_n] = \mathrm{EA(A)} + \sum_{m=0}^{n-1} D[\mathrm{A}^-(\mathrm{B})_m\cdots\mathrm{B}] - \sum_{m=0}^{n-1} D_{\mathrm{WB}}[\mathrm{A(B)}_m\cdots\mathrm{B}] \quad (1)$$

and

$$\mathrm{EA}[\mathrm{A(B)}_n] = \mathrm{EA}[\mathrm{A(B)}_{n-1}] + D[\mathrm{A}^-(\mathrm{B})_{n-1}\cdots\mathrm{B}] - D_{\mathrm{WB}}[\mathrm{A(B)}_{n-1}\cdots\mathrm{B}], \quad (2)$$

where $\mathrm{EA}[\mathrm{A(B)}_n]$ denotes the adiabatic electron affinity of the $\mathrm{A(B)}_n$ cluster, $D[\mathrm{A}^-(\mathrm{B})_m\cdots\mathrm{B}]$ is the ion–neutral dissociation energy (the absolute value of the solvation energy) for the loss of a single neutral solvent B from a given negative cluster ion, and $D_{\mathrm{WB}}[\mathrm{A(B)}_m\cdots\mathrm{B}]$ is the weak-bond dissociation energy for the loss of a single solvent B from a given neutral cluster. Since ion–solvent interaction energies generally exceed van der Waals bond strengths, it is evident from these relations that the electron affinities of clusters should increase with cluster size, and that clustering can be expected to stabilize the excess electronic charges on negative ions. Eventually, however, as the mean number of solvent neighbors interacting with the anion becomes constant, this trend should reach its limit, and cluster electron affinities will become independent of cluster size. For these reasons one expects EA values to increase relatively rapidly with cluster size for small n and then to approach a limiting value at some larger n. At still another level of refinement, one may anticipate the existence of structured EA vs n envelopes, due perhaps to unusually stable species such as those associated with filled solvation shells.

The transition $NO(X^2\Pi,\ v'=0) \leftarrow NO^-(X^3\Sigma^-,\ v''=0)$ corresponds to the (0,0) origin peak in the photoelectron spectrum of NO^- in Fig. 3. When the center-of-mass electron kinetic energy corresponding to the center of this peak is subtracted from the photon energy (2.540 eV), one obtains a nominal electron affinity for NO of 0.037 eV. Consideration of rotational and spin–orbit effects leads to a correction of -0.013 eV to this nominal value to yield the accepted value of 0.024 eV for the adiabatic electron affinity of NO.

Our interpretation of the photoelectron spectra of $NO^-(N_2O)_1$ and $NO^-(N_2O)_2$ is that they can be viewed as the spectra of NO^- ions which have been perturbed by one and by two N_2O molecules, respectively. We therefore assign peak A in the photoelectron spectrum of $NO^-(N_2O)_1$ and peak A′ in the photoelectron spectrum of $NO^-(N_2O)_2$ as the respective (0,0) origin peaks in these spectra. When the center-of-mass electron kinetic energies corresponding to the centers of peaks A and A′ are each subtracted from the photon energy, one obtains nominal electron affinities for $NO(N_2O)_1$ and $NO(N_2O)_2$ of 0.258 ± 0.009 and 0.513 ± 0.022 eV, respectively. The cited errors are just the experimental errors in the peak center determination and do not include the errors involved in correcting to the position of the origin. Making corrections to obtain the exact adiabatic electron affinities for the clusters is a difficult problem due to the manifestation of peak broadening in these photoelectron spectra. Thus, even though we maintain that peaks A and A′ correspond to the origin tran-

sitions for their respective spectra, there is no assurance that the centers of these peaks correspond to the precise locations of the origin transitions.

In addition to electron affinities, these spectra also yield ion–solvent dissociation energies. As is shown in Eq. (2), the difference between the electron affinities of two adjacent-sized clusters is equal to the dissociation energy of the larger cluster ion losing a single solvent molecule minus the weak bond dissociation energy of the larger neutral cluster losing a single solvent molecule. Since ion–solvent interaction energies are often greater than van der Waals energies by an order of magnitude, ion–solvent dissociation energies may be approximated by

$$D[A^-(B)_{n-1}\cdots B] \cong EA[A(B)_n] - EA[A(B)_{n-1}]. \quad (3)$$

This, of course, is equivalent to saying that the spectral shifts between the centers of the origin peaks of adjacent-sized cluster ions are approximately equal to the ion-solvent dissociation energy for the larger cluster ion losing a single solvent molecule. Thus, the dissociation energy for $NO^-(N_2O)_1$ breaking into NO^- and N_2O is $\sim$0.22 eV, and the dissociation energy for $NO^-(N_2O)_2$ breaking into $NO^-(N_2O)_1$ and N_2O is $\sim$0.26 eV. For reasons already stated we do not have a good measure of the uncertainty in these numbers. At this stage we take these determinations to mean that the first and second solvation energies for gas-phase nitric oxide negative ions being solvated by nitrous oxide molecules are comparable and are of the magnitude of $\sim$0.2 eV each. Guidance in appreciating these results is provided by thermochemical studies of gas-phase negative ion clustering processes.[18,19] (1) Two-tenths of an eV is a reasonable number for the solvation energy of an ion such as NO^- by a neutral such as N_2O. (2) Stepwise enthalpy changes have been measured for the addition of solvent molecules onto a variety of negative ions in which the ions' corresponding neutrals are usually species with relatively high electron affinities. Very often in negative cluster ions with large ($\sim$1 eV) first solvation energies, the second solvation energy is much smaller (often $\sim$50% of the first), while in cluster ions with first solvation energies of $\sim$0.5 eV, the second solvation energy is only slightly smaller (often by $\sim$10% of the first). In light of these trends it is not surprising that in the case of $NO^-(N_2O)_n$ where the first solvation energy is $\sim$0.2 eV, the second solvation energy is comparable.

D. Structural Implications

As noted earlier and as shown quantitatively in Table I, the photoelectron spectra of $NO^-(N_2O)_{n=1,2}$ share several similarities with the photoelectron spectrum of NO^-. The vibrational peak spacings in the NO^- spectrum are, for instance, very close to those in both $NO^-(N_2O)_{n=1,2}$ spectra. Given the broadening and the available signal in these spectra, it is difficult to discern significant differences between their spacings. Several of the peaks in the spectra of NO^-, $NO^-(N_2O)_1$, and $NO^-(N_2O)_2$ occur at similar electron kinetic energies. We believe that this is a coincidence which is caused by the similarity in the magnitudes of the NO vibrational frequency and the ion–solvent dissociation energies of $NO^-(N_2O)_{n=1,2}$, i.e., the energy shift between the spectra. We do not interpret this as resulting from unshifted yet grossly distorted NO^- Franck–Condon profiles which have persisted in the cluster ion spectra. If this were the case, one would expect to see some intensity in the cluster ion spectra at the electron energy corresponding to the (0,0) transition in the free NO^- spectrum, and one would also expect large changes in the Franck–Condon profiles of the cluster ion spectra. In point of fact, we see no discernable transitions in the cluster ion spectra at the electron energy of the (0,0) transition in free NO^-, and the Franck–Condon profiles of the cluster ion spectra are quantitatively rather similar to that of the free NO^- spectrum.

At a closer level of examination, however, small yet reproducible differences can be seen between the Franck–Condon profiles of the NO^- and the $NO^-(N_2O)_{n=1,2}$ spectra. The transitions from the $v'' = 0$ levels of the ion to the lower v' vibrational levels of the neutral state in each of the spectra in Fig. 3 grow relatively more intense with clustering. In an effort to explore the structural consequences for NO^- due to its solvation by N_2O molecules, we performed Franck–Condon analyses on the vibrational progressions in our spectra under the assumption that the cluster ion spectra could be treated as those of perturbed NO^-. We further assumed that while the bond lengths of the NO^- moieties in the cluster ions could be distorted by solvation effects, the equilibrium bond lengths of the NO moieties in the corresponding neutral clusters would remain unchanged from that of free NO. Also, the vibrational frequencies of the nitric oxide moieties were assumed to be unchanged from their free unclustered values. In this picture the perturbed NO^- potential is viewed as being energetically lowered relative to the potential of free NO^- and possibly shifted with respect to free NO^- along the bond distance coordinate. The results from these analyses found the equilibrium bond distances for NO^- and for perturbed NO^- subions in $NO^-(N_2O)_1$, and $NO^-(N_2O)_2$ to be 1.270,[49] 1.263, and 1.257 Å, respectively, indicating a small yet steady decrease in the bond length of perturbed NO^- with increasing solvation. Since the bond length changes that we have found are comparable to the uncertainties often cited in diatomic negative ion bond length determinations via this method, these results must be regarded as having come from near the edge of our technique's capabilities. Nevertheless, we believe that these results are significant deriving their credibility from the consistency with which these small Franck–Condon profile changes were observed [especially in the $NO^-(N_2O)_1$ spectrum]. Furthermore, the direction in which these changes occurred is not easily explained on the basis of variations in the electron energy analyzer's transmission function.

These results are physically reasonable. The HOMO in NO^- has antibonding character. If the excess negative charge on NO^- were diminished by its interaction with one or more N_2O molecules, then the bond length of perturbed NO^- would shrink back toward the 1.151 Å bond length of neutral NO. The NO^- bond length contraction in going from free NO^- to $NO^-(N_2O)_1$ is roughly 5% of the maximum possible contraction, i.e., the difference between the

bond lengths of free NO^- and of free NO. This is therefore a crude indicator of the extent to which the excess electron on the NO^- subion has been dispersed away from its localized charge center. Thus, even though the excess negative charge is largely localized on the NO^- subunit in $NO^-(N_2O)_n$, there is still some small degree of charge dispersal away from the primary NO^- subion. These aspects of the bonding are consistent with a Lewis acid–base interaction picture in which the NO^- subion (the base) donates some of the negative charge in its HOMO to the LUMO of N_2O. Since there is a large energy difference between the donor HOMO and the accepting LUMO, a so-called "hard–hard" acid–base interaction[50] is expected. This results in the bonding orbital of the ion–molecule complex being similar in both form and energy to the donor's HOMO with the negative charge in the complex residing mainly on the donor part of the complex.

IV. DISCUSSION

In addition to mapping the variations in cluster electron affinities and ion–solvent dissociation energies for the first two solvation steps in the $NO^-(N_2O)_n$ system, this work has also found that the cluster ion's excess negative charge is largely *localized* on one of its subunits, and that the subunit in question is NO rather than N_2O. The fact that we obtain strong evidence for the presence of $NO^-(N_2O)_n$ and no evidence for $N_2O^-(NO)_n$ is an especially intriguing result. A comparison of the relative stabilities of these two forms of the cluster ion is facilitated by the availability of values for the ion–solvent dissociation energy of $NO^-(N_2O)_1$ and the adiabatic electron affinities of NO and N_2O.[46,51] The cluster ion $NO^-(N_2O)_1$ is stabilized with respect to the free constituents $N_2O + NO + e^-$ by the adiabatic electron electron affinity of NO plus the ion–solvent dissociation energy of $NO^-(N_2O)_1$, i.e., by $\sim$0.24 eV. The combined energy of free N_2O^- and free NO is lowered with respect to the same reference by the adiabatic electron affinity of N_2O, i.e., by 0.22 eV. If the interaction between N_2O^- and NO is significantly stabilizing, then $N_2O^-(NO)_1$ will be of lower energy than $NO^-(N_2O)_1$. Such an interaction between N_2O^- and NO seems like a reasonable possibility. On the basis of electrostatics, a stabilizing interaction of a few tenths of an eV can be anticipated. In addition, both N_2O^- and NO are open shell species, and their interactions may be even stronger possibly leading to a chemical species which differs considerably from the presumed $N_2O^-(NO)_1$ solvated–ion form. Thus, on energetic grounds alone, it is surprising that we obtain evidence for only the $NO^-(N_2O)_n$ form of the cluster ion.

While it is possible that an ion derived from the interaction of N_2O^- and NO is actually formed and that its electron affinity is too high to allow photodetachment with visible photons, our observations can more likely be explained by a combination of source conditions which favor the formation of $NO^-(N_2O)_n$ over $N_2O^-(NO)_n$ and by the existence of an energy barrier between the potential minima of $NO^-(N_2O)_n$ and $N_2O^-(NO)_n$. With nitrous oxide as its feed gas, the nozzle-ion source typically produces a hundred times more NO^- than N_2O^- (see Fig. 2). Whatever the actual cluster ion production mechanism, this circumstance provides ample opportunity for the formation of $NO^-(N_2O)_n$ and relatively little chance for generating $N_2O^-(NO)_n$. A barrier is anticipated primarily because of the considerable structural differences between neutral nitrous oxide and its anion. The energy needed to bend linear N_2O to the $\sim$134° angle of N_2O^- is thought to be $\sim$1 eV or more.[52] Thus, $NO^-(N_2O)_n$ is probably produced preferentially and is then prevented from converting to the lower energy $N_2O^-(NO)_n$ -like form by the barrier. Also, even if the excess electron in $NO^-(N_2O)_1$ were to tunnel through the barrier during the $\sim 10^{-5}$ s flight time between the ion source and the photodetachment region of the apparatus, the resulting $N_2O^-(NO)_1$ would be formed near its $N_2O^- + NO$ dissociation limit. Lastly, it is interesting to note that somewhat analogous results were obtained in the infrared cryogenic studies of Milligan and Jacox[53] in which NO and N_2O were codeposited along with alkali metals (M) into argon matrices. There, evidence was found for M^+NO^- ion pairs but not for the $M^+N_2O^-$ species.

The broadening observed in these cluster ion spectra is not an instrumental artifact. It is a real effect that is more pronounced in the spectrum of $NO^-(N_2O)_2$ than in that of $NO^-(N_2O)_1$, and several mechanisms may contribute to it. Since high vibrational state densities are indigenous to cluster ions and since the internal "temperatures" of the cluster anions utilized in this work were poorly characterized, it is possible that excited weak-bond vibrations in the cluster ions may make substantial contributions to the observed broadening as weak-bond hot bands. In addition, the low-frequency vibrations in the neutral complexes that result due to photodetachment may also contribute to the broadening through Franck–Condon overlap. Furthermore, it may also happen that spectral features corresponding to the excitations of the bends and stretches of neutral N_2O solvent molecules within $NO^-(N_2O)_n$ may lie unresolved among the observed spectral progressions. We have seen a resolved manifestation of this type of transition in the photoelectron spectrum of $H^-(NH_3)_1$. There, the excitation of an ammonia stretch during the photodetachment of $H^-(NH_3)_1$ leads to a corresponding feature in the spectrum.[27] The small Franck–Condon factor for this transition implies that the ammonia solvent in $H^-(NH_3)_1$ is only slightly distorted from the structure of free or essentially free NH_3. While our $NO^-(N_2O)_{1,2}$ spectra do not show evidence for large structural distortions of the N_2O solvents, it is possible that small distortions do occur and that the ensuing transitions contribute to the broadening. Each of these mechanisms is consistent with the observed enhancement of broadening in the spectrum of $NO^-(N_2O)_2$ relative to that in the spectrum of $NO^-(N_2O)_1$. Some of the broadening may also result because of access during photodetachment to a repulsive portion of the neutral's potential surface. Contributions from this mechanism, while probably present to some degree, are expected to be relatively modest owing to the likelihood of a broad, slowly changing van der Waals-like regime on the neutral's potential surface in the region where it is sampled. We should also note that lifetime broadening due to vibrational predissociation of the nascent neutral complexes (lifetimes $\geqslant 10^{-12}$ s) would be too small to be observed at the

resolution inherent to this technique. Planned experiments which may further illuminate these issues will involve generating cooler beams of $NO^-N_2O)_n$ by using argon expansions and extending these studies to larger $NO^-(N_2O)_n$ cluster ions.

ACKNOWLEDGMENTS

We thank K. D. Jordan, W. Klemperer, and D. R. Yarkony for stimulating discussions about $NO^-(N_2O)_n$. This research was supported by the National Science Foundation under Grant No. CHE-8511320. Acknowledgment is also made to the Donors of the Petroleum Research Fund, administered by the American Chemical Society, for partial support of this work.

[1]M. J. McEwan and L. F. Phillips, *Chemistry of the Atmosphere* (Wiley, New York, 1975).
[2]*Heterogeneous Atmospheric Chemistry*, Geophysical Monograph 26, edited by D. R. Schryer (American Geophysical Union, Washington, D.C., 1982).
[3]*Electron–Solvent and Anion–Solvent Interactions*, edited by L. Kevan and B. C. Webster (Elsevier, Amsterdam, 1976).
[4]*Electrons in Fluids*, edited by J. Jortner and N. R. Kestner (Springer, New York, 1973).
[5]*Growth and Properties of Metal Clusters*, Proceedings of the 32nd International Meeting of the Societe de Chimie Physique, edited by Jean Bourdon (Elsevier, New York, 1980).
[6]M. Arshadi, R. Yamdagni, and P. Kebarle, J. Phys. Chem. **74**, 1475 (1970).
[7]J. Gaspann and K. Korting, J. Chem. Phys. **59**, 4726 (1973).
[8]J. G. Collins and P. Kebarle, J. Chem. Phys. **46**, 1082 (1967).
[9]R. Middleton, Nucl. Instrum. Methods **144**, 373 (1977).
[10]C. E. Klots and R. N. Compton, J. Chem. Phys. **69**, 1644 (1978).
[11]H. J. Kaiser, E. Heinicke, H. Baumann, and K. Bethge, Z. Phys. **243**, 46 (1971).
[12]L. Friedman and R. J. Beuhler, J. Chem. Phys. **78**, 4669 (1983).
[13]M. Armbruster, H. Haberland, and H.-G. Schindler, Phys. Rev. Lett. **47**, 323 (1981).
[14]J. F. Wilson, F. J. Davis, D. R. Nelson, R. N. Compton, and O. H. Crawford, J. Chem. Phys. **62**, 4204 (1975).
[15]L.-S. Zheng, P. J. Brucat, C. L. Pettiette, S. Yang, and R. E. Smalley, J. Chem. Phys. **83**, 4273 (1985).
[16]E. L. Quitevis, K. H. Bowen, and D. R. Herschbach, J. Phys. Chem. **87**, 2076 (1983).
[17]P. Kebarle, in *Ion–Molecule Reactions*, edited by J. L. Franklin (Plenum, New York, 1972).
[18]R. G. Keesee and A. W. Castleman, Jr., J. Phys. Chem. Ref. Data (in press).
[19]R. G. Keesee, N. Lee, and A. W. Castleman, Jr., J. Chem. Phys. **73**, 2195 (1980).
[20]D. L. Albritton, At. Data Nucl. Tables **22**, (1978).
[21]C. E. Klots and R. N. Compton, J. Chem. Phys. **69**, 1636 (1978).
[22]K. H. Bowen, G. W. Liesegang, R. A. Sanders, and D. R. Herschbach, J. Phys. Chem. **87**, 557 (1983).
[23]P. C. Cosby, J. H. Ling, J. R. Peterson, and J. T. Moseley, J. Chem. Phys. **65**, 5267 (1976).
[24]R. A. Beyer and J. A. Vanderhoff, J. Chem. Phys. **65**, 2313 (1976).
[25]A. W. Castleman, Jr., D. E. Hunton, T. G. Lindeman, and D. N. Lindsay, Intl. J. Mass Spectrum. Ion Phys. **47**, 199 (1983).
[26]S. Golub and B. Steiner, J. Chem. Phys. **49**, 5191 (1968).
[27]J. V. Coe, J. T. Snodgrass, C. B. Freidhoff, K. M. McHugh, and K. H. Bowen, J. Chem. Phys. **83**, 3169 (1985).
[28]J. V. Coe, J. T. Snodgrass, C. B. Freidhoff, K. M. McHugh, and K. H. Bowen, Chem. Phys. Lett. **124**, 274 (1986).
[29]C. R. Moylan, J. A. Dodd, and J. I. Brauman, Chem. Phys. Lett. **118**, 38 (1985).
[30]L. A. Posey, M. J. Deluca, and M. A. Johnson, Chem. Phys. Lett. **131**, 170 (1986).
[31]Y. Liu, L. Zhang, F. K. Tittel, R. F. Curl, and R. E. Smalley, J. Chem. Phys. **85**, 7434 (1986).
[32]D. G. Leopold, J. H. Ho, and W. C. Lineberger, J. Chem. Phys. **86**, 1715 (1987).
[33]H. Kistenmacher, H. Popkie, and E. Clementi, J. Chem. Phys. **61**, 5627 (1973).
[34]K. D. Jordan and J. J. Wendoloski, Chem. Phys. **21**, 145 (1977).
[35]M. D. Newton, J. Phys. Chem. **79**, 2795 (1975).
[36]J. Simons, Annu. Rev. Phys. Chem. **28**, 15 (1977).
[37]C. F. Melius, T. H. Upton, and W. A. Goddard III, Solid State Commum. **28**, 501 (1978).
[38]R. R. Corderman and W. C. Lineberger, Annu. Rev. Phys. Chem. **30**, 347 (1979).
[39]H. B. Ellis, Jr. and G. B. Ellison, J. Chem. Phys. **78**, 6541 (1983).
[40]J. V. Coe, J. T. Snodgrass, C. B. Freidhoff, K. M. McHugh, and K. H. Bowen, J. Chem. Phys. **84**, 618 (1986).
[41]H. Haberland, H.-G. Schindler, and D. R. Worsnop, Ber. Bunsenges. Phys. Chem. **88**, 270 (1984).
[42]J. L. Moruzzi and J. T. Dakin, J. Chem. Phys. **49**, 5000 (1968).
[43]J. F. Paulson, Adv. Chem. Ser. **58**, 28 (1966).
[44]P. J. Chantry, J. Chem. Phys. **55**, 2746 (1971).
[45]L. M. Branscomb, D. S Burch, S. J. Smith, and S. Geltman, Phys. Rev. **111**, 504 (1958).
[46]M. W. Siegel, R. J. Celotta, J. L. Hall, J. Levine, and R. A. Bennett, Phys. Rev. A **6**, 607 (1972).
[47]H. Hotop, R. A. Bennett, and W. C. Lineberger, J. Chem. Phys. **58**, 2373 (1973).
[48]S. B. Woo, E. M. Helmy, P. K. Mauk, and A. P. Paszek, Phys. Rev. A **24**, 1380 (1981).
[49] This is the value of $r_e''(NO^-)$ that we obtained from a Franck–Condon analysis of the vibrational progression in our photoelectron spectrum of NO^-. Previous values include $r_e''(NO^-) = 1.258$ Å from Ref. 46 and $r_e''(NO^-) = 1.267$ Å from D. Teillet-Billy and F. Fiquet-Fayard, J. Phys. B **10**, L111 (1977).
[50]G. Klopman, J. Am. Chem. Soc. **90**, 223 (1968).
[51]D. G. Hopper, A. C. Wahl, R. L. C. Wu, and T. O. Tiernan, J. Chem. Phys. **65**, 5474 (1976).
[52]E. E. Ferguson, F. C. Fehsenfeld, and A. L. Schmeltekopf, J. Chem. Phys. **47**, 3085 (1967).
[53]D. E. Milligan and M. E. Jacox, J. Chem. Phys. **55**, 3404 (1971).